Available online at www.sciencedirect.com
SCIENCE DIRECT®
Physics Letters B 624 (2005) 195–202
PHYSICS LETTERS B
www.elsevier.com/locate/physletb

Low-energy dipole excitations towards the proton drip-line: Doubly magic ^{48}Ni

N. Paar, P. Papakonstantinou, V.Yu. Ponomarev [1], J. Wambach

Institut für Kernphysik, Technische Universität Darmstadt, Schlossgartenstrasse 9, D-64289 Darmstadt, Germany

Received 19 May 2005; received in revised form 20 July 2005; accepted 12 August 2005

Available online 24 August 2005

Editor: J.-P. Blaizot

Abstract

The properties of the low-energy dipole response are investigated for the proton-rich doubly magic nucleus ^{48}Ni, in a comparative study of two microscopic models: fully self-consistent relativistic random-phase approximation (RRPA) based on the novel density-dependent meson-exchange interactions, and continuum random-phase approximation (CRPA) using Skyrme-type interactions with the continuum properly included. Both models predict the existence of the low-energy soft mode, i.e., the proton pygmy dipole resonance (PDR), for which the transition densities and RPA amplitudes indicate the dynamics of loosely bound protons vibrating against the rest of the nucleons. The CRPA analysis indicates that the escape width for the proton PDR is rather large, as a result of the coupling to the continuum.

PACS: 21.10.Gv; 21.30.Fe; 21.60.Jz; 24.30.Cz

One of the major challenges in the region of unstable nuclei is the understanding of soft modes of excitations which involve loosely bound nucleons, nucleon halo, or skin. In particular, in neutron-rich nuclei, nucleons from the neutron skin may give rise to a low-energy dipole mode, known as a pygmy dipole resonance (PDR) [1]. Some experimental evidence about the low-lying dipole excitation phenomena in neutron-rich nuclei is available from (i) electromagnetic excitations in heavy-ion collisions [2], and (ii) nuclear resonance fluorescence experiments for nuclei with moderate neutron to proton number ratios, e.g., ^{116,124}Sn [3], ^{138}Ba [4], Pb [5], and Ca [6] isotopes, and $N = 82$ isotones [7]. On the other side, a variety of theoretical models have in recent years been employed in studies of the low-lying E1 strength: continuum quasiparticle RPA formulated in the coordinate-space Hartree–Fock–Bogoliubov framework [8], continuum RPA with Woods–Saxon potential for the ground

E-mail address: nils.paar@physik.tu-darmstadt.de (N. Paar).
[1] Permanent address: Joint Institute of Nuclear Research, Dubna, Russia.

0370-2693/$ – see front matter
doi:10.1016/j.physletb.2005.08.043

state and Landau–Migdal force in the residual interaction [9], the time-dependent density-matrix theory [10], Skyrme–Hartree–Fock + quasiparticle RPA with phonon coupling [11,12], and the quasiparticle-phonon model [3,5,13]. In the relativistic framework, properties of low-energy excitations have been systematically studied in the relativistic RPA (RRPA) [14], and the relativistic quasiparticle RPA (RQRPA) [15–18]. Both experimental and theoretical studies qualitatively agree on the global properties of the isovector dipole response, i.e., as the number of neutrons increases along the isotope chain, the transition strength distribution is characterized by the appearance of pronounced low-lying E1 strength. Within the relativistic R(Q)RPA studies, it has been shown in a fully self-consistent way that the low-lying pygmy state represents a genuine structure effect: the neutron skin oscillates against the core, exhibiting a collective nature from medium towards heavier nuclei [14,15]. A detailed quantitative description of the low-lying E1 strength in neutron-rich nuclei is essential for calculations of radiative neutron capture rates in the r-process, and elemental abundances from nucleosynthesis [19].

The structure of nuclei on the proton-rich side is equally important for revealing many aspects of the underlying many-body problem and properties of the effective nuclear interactions. At the same time, a quantitative description of proton-rich nuclei is of a particular importance for describing the rapid proton capture process of nucleosynthesis. Proton-rich nuclei are characterized by unique ground-state properties such as β decays with large Q values, and direct emission of charged particles. The two-proton ground state radioactivity has recently been observed as a decay mode of ^{45}Fe [20,21]. At the present time, knowledge on dipole excitations in nuclei towards the proton drip-line is rather limited. Only very recently, the first microscopic theoretical prediction of the proton pygmy dipole resonance has been indicated in the framework of RQRPA based on the relativistic Hartree–Bogoliubov model (RHB) [22]. For nuclei close to the proton drip-line, the model calculations predicted the occurrence of pronounced dipole peaks below 10 MeV in excitation energy, due to collective vibrations of loosely-bound protons against the proton–neutron core.

In this Letter, we employ two theoretical approaches in a comparative study of the low-lying E1 strength of the proton-rich nucleus ^{48}Ni: the fully self-consistent relativistic RPA (RRPA) based on novel density-dependent interactions, and the continuum RPA (CRPA) with Skyrme-type interactions. An essential objective of this study is to ensure that the proton PDR is inherent for different models, based on different assumptions and effective interactions, and to quantify the global properties of this mode, i.e., excitation energies and B(E1) strength, which may also be interesting for the future experimental studies. Furthermore, we employ the CRPA model to investigate the role of the coupling to the continuum for the proton PDR. We choose to analyse a doubly magic nucleus ^{48}Ni, which is the most proton-rich isotope that has been experimentally discovered [23]. For comparison, we also present results for ^{56}Ni, which lies close to the valley of stability. Being doubly magic, these two isotopes can be studied within the CRPA and RRPA models, which do not include pairing correlations. Ground state properties of proton-rich nuclei around ^{48}Ni have extensively been studied within the shell-model [24], Hartree–Fock–Bogoliubov [25], and relativistic Hartree–Bogoliubov (RHB) theory [26]. Proton drip-line nuclei are characterized by a reduction of the spin–orbit term of the effective interaction, outer orbits appear to be very weakly bound, and the Fermi energy level may become positive. Due to the presence of the Coulomb barrier, loosely bound orbits are stabilised, in contrast to the neutron drip-line nuclei where the weakly bound neutron orbits are more spatially extended. The interplay of all these effects in the nuclear ground state will shape the properties of the corresponding dipole excitation response.

In the following, we briefly present the basic theoretical background of the Dirac–Hartree + RRPA and Skyrme–Hartree–Fock + CRPA models and their effective interactions.

In recent years, the relativistic mean-field theory and linear response based on density-dependent interactions, turned out to be very successful in studies of nuclear ground-state properties and excitation phenomena with a minimal set of parameters in a fully microscopic way [27]. Within this framework, the nucleus is described as a system of Dirac nucleons which interact in a relativistic covariant manner by exchange of effective mesons. The model is formulated with the Lagrangian density which explicitly includes the

density dependence in σ, ω, and ρ meson–nucleon vertices. In the present study, we employ the density-dependent effective interactions which are constrained by the properties of finite nuclei and nuclear matter: DD-ME1 [28], and the new interaction DD-ME2 which provides an improved description of the isovector dipole response [29]. In the small-amplitude limit, the RRPA equations are derived from the equation of motion for the nucleon density [30]. Both in RRPA and CRPA models, we use the same form of the effective isovector dipole operator as in Ref. [22]. The RRPA configuration space is constructed from particle–hole (ph) pairs composed of the particle states above the Fermi level, and hole states in the Fermi sea. In addition, in the relativistic case, one also needs to include transitions to unoccupied states from the Dirac sea [27]. The resulting RRPA discrete spectra are averaged with the Lorentzian distribution which includes an arbitrary choice for the width, $\Gamma_{\mathrm{RRPA}} = 1$ MeV. The Dirac–Hartree + RRPA model is fully self-consistent, i.e., both the equations of the ground state, and the residual RPA interaction are derived from the same effective Lagrangian. This is an essential property for an accurate decoupling of the spurious center-of-mass motion without need for including any additional free parameters. For the present study we use the Dirac–Hartree model formulated in the harmonic oscillator basis. Within this approach, the particle continuum is represented by a set of discrete states, which are used to construct the RRPA configuration space. In Ref. [26] it has been verified that for nuclei towards the proton drip-line, an expansion in a large oscillator basis ($N = 20$) provides sufficiently accurate solutions, in complete agreement with the model formulated in the coordinate space.

The second theoretical framework for the present Letter is the Skyrme–Hartree–Fock (SHF) plus continuum-RPA (CRPA) model. The HF equations describing the ground state are derived variationally from the Skyrme energy functional. The ph residual interaction is derived from the same energy functional. In the present study, the Coulomb interaction, as well as spin-dependent terms are omitted from the residual interaction. The CRPA is formulated in the coordinate space, and the particle continuum is fully taken into account. The transition strength distribution $R(E)$ is continuous by construction. A small but finite value of $\mathrm{Im}\, E \equiv \Gamma/2$ entering the evaluation of the ph Green function ensures that bound transitions acquire a finite width and thereby contribute to the distribution. More details on the CRPA model can be found in Refs. [31, 32] and references therein.

For the purposes of the present Letter we implement various parameterisations of the Skyrme interaction, corresponding to different nuclear-matter properties. In particular, they have different (isoscalar) effective mass m^*/m and isovector effective mass m^*_v/m. These quantities have influence on the evaluated properties of the isovector giant dipole resonance (IVGDR) [19,33] and the low-energy dipole transitions. In general, interactions with a high effective mass are not able to reproduce the IVGDR properties. However, a high m^*/m may be more appropriate to describe correctly the density of states lying close to the Fermi energy, which are relevant for the present study. Therefore, we use several different parameterisations of the Skyrme interaction, in order to ensure the general validity of our conclusions, at least on a qualitative level. We employ parameterisation MSk7 ($m^*/m = m^*_v/m = 1.05$), based on a Hartree–Fock–BCS model [34], and two interactions from the recent BSk series, namely BSk8 [35] ($m^*/m = 0.80$, $m^*_v/m = 0.87$) and BSk2 ($m^*/m = 1.04$, $m^*_v/m = 0.86$) [36]. Both BSk interactions were parameterised by fitting the values of nuclear masses calculated within the Hartree–Fock–Bogoliubov method to essentially all the measured ones. We also use the traditional parameterisation SkM* ($m^*/m = 0.786$, $m^*_v/m = 0.875$) [37], which was extensively used in previous studies of giant resonances and response of exotic nuclei, e.g., Refs. [31,32,38,39].

Next, we present the results obtained with the two models. In Fig. 1 we plot the ground-state proton and neutron density distributions for ^{48}Ni and ^{56}Ni, calculated with Dirac–Hartree and SHF models, based on the DD-ME1 and BSk8 effective interactions, respectively. For ^{56}Ni ($Z = 28$, $N = 28$) the proton and neutron density distributions are similar in the nuclear interior and beyond the surface region the differences completely vanish. However, in the case of ^{48}Ni ($Z = 28$, $N = 20$), due to the excess of loosely-bound protons, the proton density distribution is considerably extended beyond the neutron density distribution. This effect is especially pronounced at radial distances $r > 2$ fm, and it resembles in structure a proton skin. Due to the presence of the Coulomb barrier, which

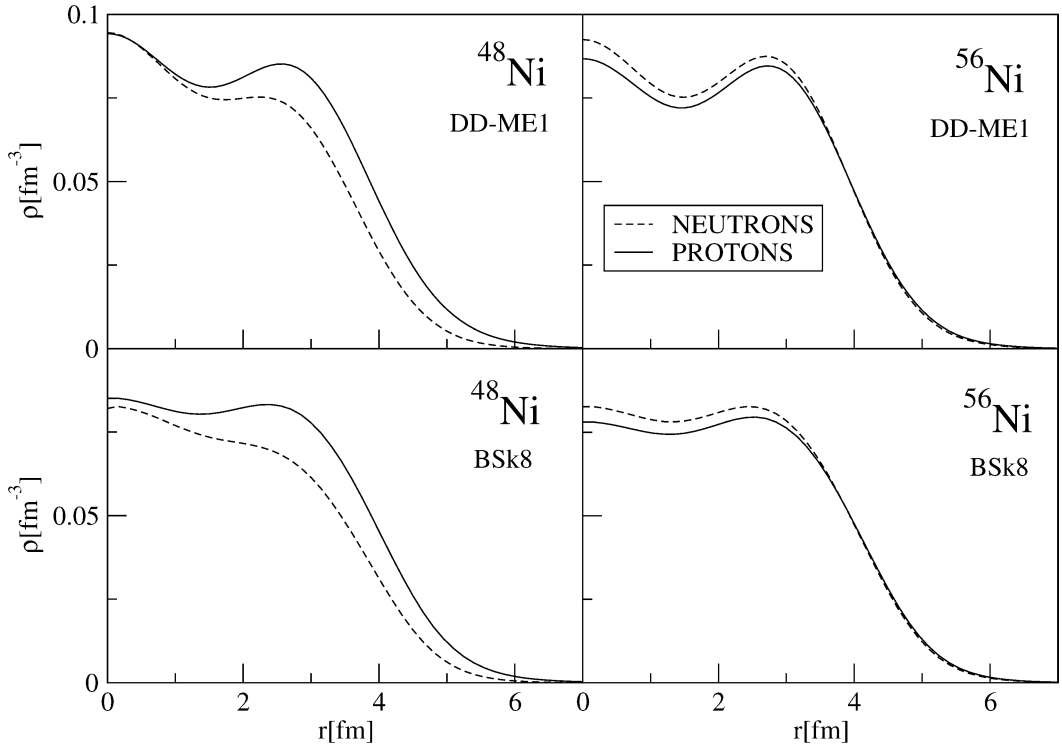

Fig. 1. Proton and neutron ground-state density distributions for ^{48}Ni and ^{56}Ni calculated with the Dirac–Hartree (DD-ME1 interaction) and Skyrme–Hartree–Fock (BSk8 interaction) models.

tends to localise protons within the nuclear interior, the proton skin is not so pronounced an effect as the neutron skin. However, some evidence for increasing of the proton-skin thickness in nuclei towards the proton drip-line is provided both by theoretical and by experimental studies [25,40].

In Fig. 2 we present results obtained within the fully self-consistent RRPA model based on Dirac–Hartree ground state with DD-ME1 effective interaction. In the left panel we display the isovector dipole strength distributions for ^{48}Ni and ^{56}Ni. In the region of the isovector giant dipole resonance (IVGDR), the difference between the two distributions is very small and mainly consists of small fluctuations of the IVGDR tail. In agreement with the mass dependence of the giant resonance, the distribution of ^{48}Ni is only slightly pushed to higher energies from the one for ^{56}Ni. However, in the low-energy region, the E1 strength distributions are rather different: whereas there are no low-lying states for ^{56}Ni, proton-rich ^{48}Ni is characterized by the appearance of a pronounced amount of low-lying transition strength. In order to clarify the origin of this strength, in the right panel of Fig. 2 we show the neutron and proton transition densities for two characteristic peaks: the low-lying state at 7.72 MeV, and the giant resonance state at 18.71 MeV. The transition densities of the latter display the dynamics of IVGDR: collective oscillation of neutrons against protons. For the low-energy peak, however, the proton and neutron transition densities are in phase in the nuclear interior, whereas beyond the surface region there are no contributions from the neutrons and proton transition density dominates. This type of nuclear dynamics is characteristic for the proton PDR, where loosely bound protons oscillate against the rest of the nucleons [22], in analogy to the neutron PDR in neutron-rich nuclei. The RRPA amplitudes for the E1 state at 7.72 MeV reveal the structure of the proton PDR in detail: the main contribution to the strength of the peak consists of transitions from the proton $1f_{7/2}$ state, which is located at 0.11 MeV and weakly bound partly due to the presence of the Coulomb bar-

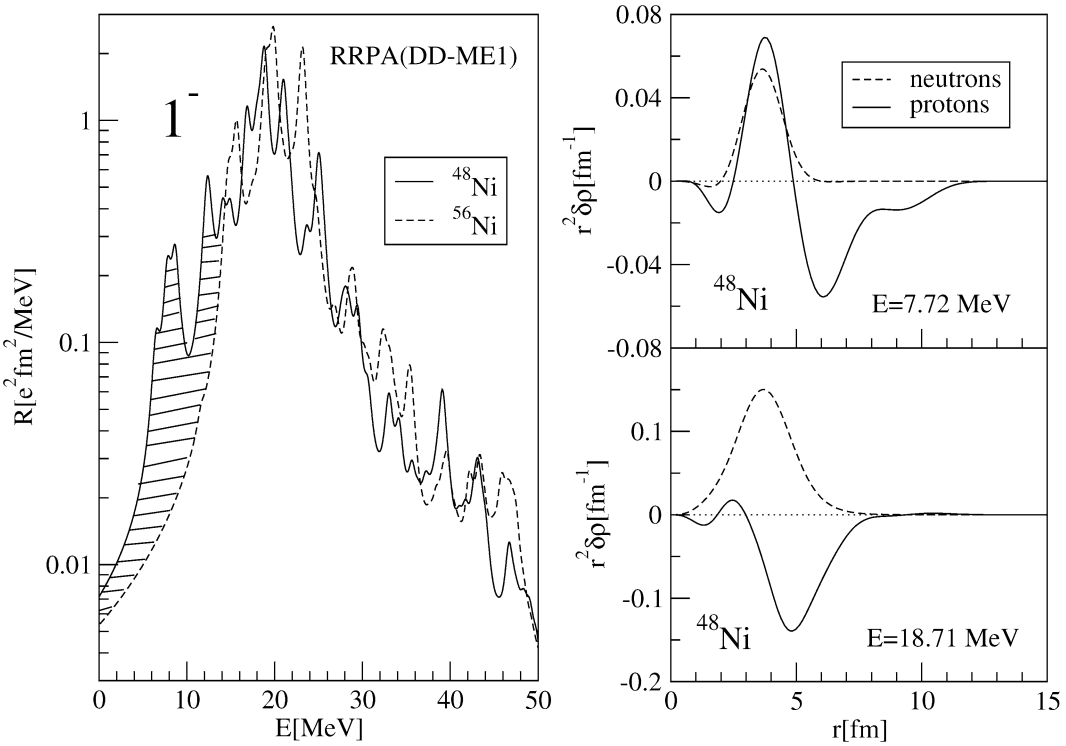

Fig. 2. The Dirac–Hartree + RRPA isovector dipole strength distribution for ^{48}Ni and ^{56}Ni (left panel). The proton and neutron transition densities are displayed for the low-lying state ($E = 7.72$ MeV) and isovector giant resonance ($E = 18.71$ MeV). The DD-ME1 effective interaction is employed. The shaded area denotes the difference between the low-energy part of the strength distributions of ^{48}Ni and ^{56}Ni.

rier. The contributions from other transitions are at least an order of magnitude smaller. Therefore, the appearance of the low-lying proton PDR strength is directly related to the pronounced proton density distributions from Fig. 1. Protons from the same loosely-bound orbit contribute to the exotic nuclear structure of the ground state, and to the excitation phenomena of the proton PDR. The collectivity of the proton PDR peak considerably increases in open shell-nuclei, due to the increased number of two-quasiparticle configurations composed from many states around the Fermi surface which are, in that case, partially occupied [22].

The properties of the low-lying dipole transition strength are strongly sensitive on the proton excess. In comparison of the cases of ^{46}Fe (from Ref. [22]) and ^{48}Ni (DD-ME1 interaction is employed in both cases), one can see that the GDR peak energy only weakly changes (0.2 MeV) with addition of two more protons. The peak energies of the proton PDR mode, however, lowers from 9.4 MeV towards 7.7 MeV for ^{46}Fe and ^{48}Ni, respectively. Obviously, the properties of the low-lying dipole transition strength are more sensitive to the variations of the nucleon excess than GDR. This type of behaviour indicates the nature of the proton PDR mode: as the number of protons increases, the oscillations of loosely-bound protons acquire lower frequencies due to their weaker binding.

By using the Skyrme–Hartree–Fock+CRPA model with BSk8 effective interaction, we repeat the same study of the isovector dipole transition strength for ^{48}Ni and ^{56}Ni isotopes. In the left panel of Fig. 3, we notice that for the two Ni isotopes the strength distributions are not very different for $E > 10$ MeV. In agreement with the RRPA results, the CRPA low-lying transition strength for ^{48}Ni is strongly enhanced in comparison with the ^{56}Ni case. In the right panel of Fig. 3 we plot the transition densities for a low energy peak at 9.72 MeV and the IVGDR at 20.28 MeV. The displayed CRPA transition densities are in full agree-

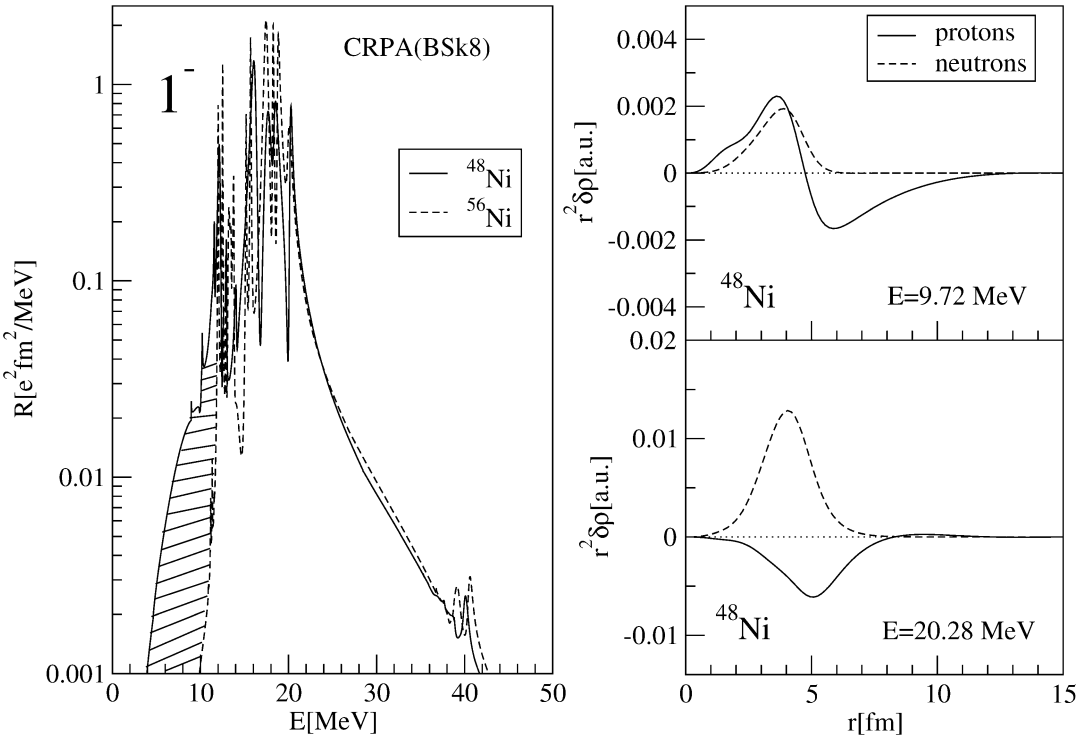

Fig. 3. Same as in Fig. 2, but calculated with the Skyrme–Hartree–Fock + CRPA model by using BSk8 effective interaction. Transition densities are shown for the states with $E = 9.72$ and 20.28 MeV.

ment with the RRPA calculations, i.e., the high-energy peak corresponds to the collective IVGDR where protons oscillate versus neutrons, while the low-lying transitions reveal the nature of the proton PDR.

Within the CRPA model, we do not obtain only one pronounced low-energy PDR peak for ^{48}Ni, but rather a smooth continuum, slightly structured around 9–10 MeV. One of the structures is the 9.72 MeV peak for which the transition density was plotted in Fig. 3. This continuum is not an artifact of the small smearing parameter used, $\Gamma = 0.05$ MeV. The particle threshold energy is $E_{\rm th} = 3.3$ MeV. We have evaluated the proton- and neutron-transition densities corresponding to various values of excitation energy below $E =$ 10 MeV, and verified that they are characterized by transitions of a similar nature as the 9.72 MeV peak. The above discussion remains valid qualitatively when other Skyrme interactions are used. More numerical results are presented below.

In Table 1 we compare the global properties of the proton PDR for ^{48}Ni, obtained using the RRPA model with DD-ME1 and DD-ME2 effective interactions, and the CRPA model with Skyrme interactions BSk8, BSk2, MSk7 and SkM*. We have calculated the summed low-lying strength m_0, the energy-weighted strength m_1 and the centroid energy m_1/m_0 for excitation energies below 10 MeV, where m_k corresponds to the kth moment of the strength distribution. Since the CRPA strength distribution is continuous in this region, the choice of the cut-off value of PDR region at 10 MeV is somewhat arbitrary and the definition of the centroid energy becomes ambiguous. For this reason, the respective results are placed inside brackets. In addition, we list the relative amount of the low-lying strength m_1 with respect to the classical Thomas–Reiche–Kuhn sum rule TRK $=$ $14.9 \cdot (NZ/A)\, e^2$ fm^2 MeV. The centroid energies of the proton PDR for ^{48}Ni are obtained around 8 MeV. The two different models are in fair agreement for various interactions, exhausting for the proton PDR from $\approx 0.9\%$ (BSk8) towards $\approx 1.6\%$ (DD-ME1, MSk7) of the classical TRK sum rule.

Table 1
The low-lying ($E < 10$ MeV) dipole transition strength (m_0), energy-weighted low-lying strength (m_1), its fraction of the classical TRK sum rule, centroid energies and widths (σ) for ^{48}Ni, calculated with RRPA (DD-ME1 and DD-ME2 effective interactions) and CRPA (BSK8, BSK2, MSk7 and SkM* Skyrme effective interactions) models. The definition of the centroids and widths in the CRPA model is somewhat ambiguous (see text) and therefore the corresponding values are given in square brackets

	DD-ME1	DD-ME2	BSk8	BSk2	MSk7	SkM*
m_0 [e^2 fm^2]	0.346	0.336	0.201	0.259	0.352	0.179
m_1 [e^2 fm^2 MeV]	2.783	2.718	1.632	2.132	2.914	1.485
m_1/TRK [%]	1.60	1.56	0.94	1.23	1.67	0.85
m_1/m_0 [MeV]	8.03	8.08	[8.10]	[8.22]	[8.28]	[8.30]
σ [MeV]	0.77	0.79	[1.42]	[1.45]	[1.48]	[1.40]

We found that BSk8 and SkM* gave the lowest values of low-lying PDR strength. In general, the Skyrme-type interactions with the lower value of m^*/m, result in weaker low-energy transition strength. The amount of the low-lying strength is directly related to the energy e_f of the least bound proton single-particle state $1f_{7/2}$ and the particle threshold energy E_{th}. For ^{48}Ni, these quantities are as follows: $e_f = -0.88$ MeV and $E_{\text{th}} = 4.2$ MeV for SkM*, $e_f = -0.03$ MeV and $E_{\text{th}} = 3.3$ MeV for BSk8, $e_f = 0.26$ MeV and $E_{\text{th}} = 3.0$ MeV for BSk2, and $e_f = 0.35$ MeV and $E_{\text{th}} = 3.0$ MeV for MSk7. As the energy of $1f_{7/2}$ proton state changes to higher values, the corresponding low-lying E1 strength is more enhanced. It is surprising that the Skyrme interaction whose effective-mass properties differ the most from the ones of the relativistic forces, namely MSk7, gives the best agreement with the RRPA results. The opposite holds for BSk8 and SkM*, whose properties differ the least from the ones of the relativistic forces. We notice, moreover, that the BSk2 corresponds to almost as large an effective mass m^*/m as the MSk7, and practically the same E_{th}, yet its predictions for the PDR are closer to the BSk8. Its isovector effective mass, though, is low and almost the same as BSk8. Within the present CRPA model, a Skyrme interaction cannot provide as much low-lying strength as the RRPA model, unless a high value of isovector effective mass is used. It is an interesting trend, but it cannot be established only by the study of a single nucleus. Finally, there does not seem to exist a correlation between the degrees of quantitative agreement of the RRPA and CRPA models on the properties of the PDR on one hand, and the e_f value on the other. The absolute difference between the value of e_f corresponding to the Skyrme force MSk7 (best agreement with RRPA on PDR strength) and the RRPA result, 0.11 MeV, is almost as large as in the case of the SkM* (the worst agreement).

In the last row of Table 1, we show an estimate of the PDR width, given by the mean deviation of the strength distribution up to 10 MeV, $\sigma = \sqrt{(m_2/m_0) - (m_1/m_0)^2}$. Different Skyrme interactions result in similar widths, $\sigma \approx 1.4$ MeV. On the other side, the width evaluated from the RRPA discrete strength distribution with the DD-ME1 interaction with a smaller effective mass, results in $\sigma = 0.77$ MeV. In the RRPA case it provides only a measure of the fragmentation of the low-lying strength, and therefore, it is smaller in comparison with the CRPA width which includes the contributions of the continuum.

In conclusion, we have studied the low-lying dipole response of a representative case of a proton dripline nucleus, namely the doubly magic ^{48}Ni. We have employed two different microscopic models, Dirac–Hartree + RRPA, and Skyrme–Hartree–Fock + CRPA, with various effective interactions. Within the latter approach, a proper treatment of the particle continuum is included, enabling us to study the relevance of the continuum for the low-lying strength. The comparison of E1 strength distributions for ^{48}Ni and ^{56}Ni, and transition densities, show that the low-lying dipole strength is a fundamental property of the proton-rich nuclei, and it corresponds to the proton pygmy dipole resonance, where loosely bound protons vibrate against the approximately isospin-saturated proton-neutron core. The coupling to the particle continuum results in an enhanced width of the proton PDR mode, estimated around 1.4 MeV. However, it remains unresolved why the best agreement on the proton PDR

properties, between the relativistic and nonrelativistic models, is obtained for DD-ME1 and MSk7 interactions which have quite different properties. Whereas DD-ME1 represents an advanced density-dependent interaction appropriate for the studies of both stable and exotic nuclei, MSk7 has large isoscalar and isovector effective mass, and its properties were recently improved in BSk series. A consistent comparison would necessitate a proper inclusion of the continuum in the RRPA model, and on the other side, a fully self-consistent CRPA model without neglecting of terms in the residual interaction. Nevertheless, we have shown that the two different models agree fairly well on the global properties of the proton PDR, and provide a clear theoretical picture for its underlying nature. We hope that the future experimental studies towards the proton drip-line will provide evidence for this exotic mode.

Acknowledgements

This work has been supported by the Deutsche Forschungsgemeinschaft (DFG) under contract SFB 634.

References

[1] Y. Suzuki, K. Ikeda, H. Sato, Prog. Theor. Phys. 83 (1990) 180.
[2] A. Leistenschneider, et al., Phys. Rev. Lett. 86 (2001) 5442.
[3] K. Govaert, et al., Phys. Rev. C 57 (1998) 2229.
[4] R.D. Herzberg, et al., Phys. Rev. C 60 (1999) 051307.
[5] J. Enders, et al., Nucl. Phys. A 724 (2003) 243.
[6] T. Hartmann, et al., Phys. Rev. Lett. 93 (2004) 192501.
[7] A. Zilges, et al., Phys. Lett. B 542 (2002) 43.
[8] M. Matsuo, Nucl. Phys. A 696 (2001) 371.
[9] T.N. Leite, N. Teruya, Eur. Phys. J. A 21 (2004) 369.
[10] M. Tohyama, A.S. Umar, Phys. Lett. B 516 (2001) 415.
[11] G. Coló, P.F. Bortignon, Nucl. Phys. A 696 (2001) 427.
[12] D. Sarchi, P.F. Bortignon, G. Coló, Phys. Lett. B 601 (2004) 27.
[13] N. Tsoneva, H. Lenske, Ch. Stoyanov, Phys. Lett. B 586 (2004) 213.
[14] D. Vretenar, N. Paar, P. Ring, G.A. Lalazissis, Nucl. Phys. A 692 (2001) 496.
[15] N. Paar, P. Ring, T. Nikšić, D. Vretenar, Phys. Rev. C 67 (2003) 034312.
[16] L.G. Cao, Z.Y. Ma, Mod. Phys. Lett. A 19 (2004) 2845.
[17] N. Paar, T. Nikšić, D. Vretenar, P. Ring, Phys. Lett. B 606 (2005) 288.
[18] N. Paar, T. Nikšić, D. Vretenar, P. Ring, Int. J. Mod. Phys. E 14 (2005) 29.
[19] S. Goriely, E. Khan, M. Samyn, Nucl. Phys. A 739 (2004) 331.
[20] J. Giovinazzo, et al., Phys. Rev. Lett. 89 (2002) 102501.
[21] M. Pfutzner, et al., Eur. Phys. J. A 14 (2002) 279.
[22] N. Paar, D. Vretenar, P. Ring, Phys. Rev. Lett. 94 (2005) 182501.
[23] B. Blank, et al., Phys. Rev. Lett. 84 (2000) 1116.
[24] W.E. Ormand, Phys. Rev. C 53 (1996) 214.
[25] W. Nazarewicz, et al., Phys. Rev. C 53 (1996) 740.
[26] D. Vretenar, G.A. Lalazissis, P. Ring, Phys. Rev. C 57 (1998) 3071.
[27] D. Vretenar, A.V. Afanasjev, G.A. Lalazissis, P. Ring, Phys. Rep. 409 (2005) 101.
[28] T. Nikšić, D. Vretenar, P. Finelli, P. Ring, Phys. Rev. C 66 (2002) 024306.
[29] G.A. Lalazissis, T. Nikšić, D. Vretenar, P. Ring, Phys. Rev. C 71 (2005) 024312.
[30] T. Nikšić, D. Vretenar, P. Ring, Phys. Rev. C 66 (2002) 064302.
[31] P. Papakonstantinou, J. Wambach, E. Mavrommatis, V.Yu. Ponomarev, Phys. Lett. B 604 (2004) 157.
[32] P. Papakonstantinou, E. Mavrommatis, J. Wambach, V.Yu. Ponomarev, J. Phys. G 31 (2005) 185.
[33] P.-G. Reinhard, Nucl. Phys. A 649 (1999) 305c.
[34] S. Goriely, F. Tondeur, J.M. Pearson, At. Data Nucl. Data Tables 77 (2001) 311.
[35] M. Samyn, S. Goriely, M. Bender, J.M. Pearson, Phys. Rev. C 70 (2004) 044304.
[36] S. Goriely, M. Samyn, P.-H. Heenen, J.M. Pearson, F. Tondeur, Phys. Rev. C 66 (2002) 024326.
[37] J. Bartel, P. Quentin, M. Brack, C. Guet, H.-B. Hakansson, Nucl. Phys. A 386 (1982) 79.
[38] I. Hamamoto, H. Sagawa, X.Z. Zhang, Phys. Rev. C 56 (1997) 3121.
[39] I. Hamamoto, H. Sagawa, X.Z. Zhang, Phys. Rev. C 57 (1998) 1064.
[40] A. Ozawa, et al., Nucl. Phys. A 709 (2002) 60.